Supplementary Information:

Streptavidin binding as a model to characterize thiol-ene chemistry based polyamine surfaces for reversible photonic protein biosensing

Eva Melnik[1], Paul Muellner[1], Ole Bethge[2], Emmerich Bertagnolli[b], Rainer Hainberger[1], Michael Laemmerhofer[3]

[1] *AIT Austrian Institute of Technology GmbH, Health & Environment Department, Molecular Diagnostics, 1220 Vienna, Austria*

[2] *Institute for Soli-State Electronics, Vienna University of Technology, Floragasse 7, 1040 Vienna, Austria*

[3] *University of Tübingen, Institute of Pharmaceutical Sciences, Auf der Morgenstelle 8, Tübingen, Germany*

Table of Contents:

1 Materials

(3-Mercaptopropyl)trimethoxysilane (MPTMS), ethylenediamine (EDA) hydrochloride, 2-(N-morpholino)ethanesulfonic acid (MES), Sulfo-N-hydroxysulfosuccinimide (Sulfo-NHS), 2,2-dimethoxy-2-phenylacetophenone (DMPA), Tetramethylrhodamine-5-maleimide (TMR5M), poly(amido)amine (PAMAM) dendrimer G1, Polyethyleneimine (PEI, 750 kDa), phosphate buffer saline (PBS) 15 mM, streptavidin and bovine serum albumin were purchased from Sigma-Aldrich (Vienna, Austria). 10-Undecenoic acid (UDA) was from Merck Chemicals (Darmstadt, Germany). NHS-DyLight, NHS-biotin, EZ-Link NHS-iminobiotin and 1-ethyl-3-(3-dimethylaminopropyl)carbodiimide (EDC) were purchased from Pierce (supplied by ThermoFisher, Vienna, Austria). The PAMAM G5 was obtained from Starpharma (Melbourne, Australia).

2 Instruments

Fluorescence scanner

Fluorescence scans were performed with the ArrayPro® TECAN fluorescence scanner from Media Cybernetics in Bethesda, USA with 532 nm (or 633 nm) excitation wavelength and 575 nm (or 692 nm) emission filter. For fluorescence intensity measurements the open access software ImageJ was used for data processing.

UV-crosslinker

For the photo-induced thiol-ene click reaction a UV-crosslinker (CL-1000L,UVP, Upland, California, USA) with 365 nm wavelength and 6 mW/cm^2 irradiation intensity was utilized.

X-ray photoelectron spectroscopy (XPS)

X-ray photoelectron spectra were obtained by using a system with a Phoibos 150 MCD-9 detector from SPECS Surface Nano Analysis GmbH (Berlin, Germany) equipped with a magnesium X-ray source (1253 eV emission line). Take-off angle between detector and sample was set to 0°. In order to derive information on the bonding states of the atoms, the individual atom peaks from the XPS spectra were deconvoluted by using the software CasaXPS (Version 2.3.15). All spectra were calibrated in respect to the carbon 1s state and consistency of the spectra was proven by using the Au atomic states.

MZI-measurement setup

Hydrogenated amorphous silicon based Mach-Zehnder interferometric (a-Si:H MZI) sensors were used for photonic sensing. A tunable laser with a central wavelength of 1310 nm acted as light source and the in and out coupling was done by end-face coupling from optical fibers. In the a-Si:H MZI sensor the light propagating in the input rib waveguide is split into two optical paths, the measurement

and the reference arm, by means of a Y-junction. After a distance of 10 mm the light from these two arms is recombined again by another Y-junction (see Fig. S1 A)).

The reference arm of the MZI is covered with a cladding layer (SU-8), so that binding events on the sensor surface can only influence the propagation of the waveguide mode in the measurement arm, which subsequently leads to a sinusoidal modulation of the output signal as function of the effective index of the measurement arm at the end of the interferometer (see equation (1)). In this equation, the recorded output power normalized to P_{in} (P_{out}/P_{in}) is a function of the measurement window length *(L)*, the wave number in vacuum (k_0) and the difference of the effective indices (Δn_{eff}) between the measurement and the reference arm.

$$\frac{P_{out}}{P_{in}} = \frac{1}{2}\left[1 + \cos(\Delta n_{eff} L k_0)\right] \qquad \text{(Eq. 1)}$$

During the target protein measurement on an a-Si:H MZI sensor, a protein layer accumulate at the surface (see Fig. S1 B)). Due to the evanescent wave sensing principle the refractive index change and the thickness of the protein layer accumulation, lead to an increase of the effective index difference [1,2] between the measurement and the reference arm. This increase can be measured as modulation of the optical output power, from which the accumulated phase shift ($\Delta\Phi=\Delta n_{eff} L k_0$) is calculated that correlates with the amount of target molecules captured on the surface.

In order to enable the measurement of target proteins in liquid, a PDMS fluidic chamber was mounted on top of the sensor. The MZI-sensor measurement setup was fully equipped and consisted of an optical measurement station and a fluidic control system (up to five different liquids can be used) with an electronically controlled host-syringe pump system (flow rate: 20 µl/min). These components were operated by a single control software. Our measurement setup is highly stable and we have performed real-time monitoring of deposition of protein layers over a period of up to 8h [3].

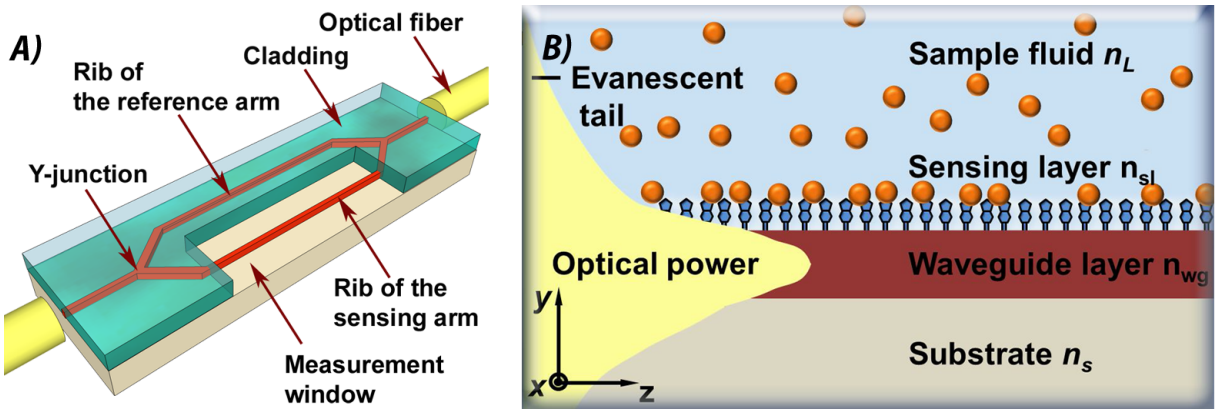

Figure S1: A) MZI structure; B) Evanescent wave based sensing principle: binding of biomolecules to sensing arm induce a local refractive index change at the surface, which changes the phase velocity of the light propagation in the waveguide.

3 Experimental Procedures

Control samples and MZI sensors fabrication

The crystalline silicon (cSi) control samples were prepared by cleaving a silicon wafer in 2x2 cm^2 pieces. The silicon wafers (purchased from Soitec, Bernin, France) consist of 2000 nm silicon dioxide as substrate and 220 nm undoped silicon (crystallographic orientation <100>). The cleaved cSi control samples were cleaned in pyranha solution (3:1 sulfuric acid:hydrogen peroxide) for five minutes, washed with ultrapure water and 2-propanol, and finally dried in the nitrogen stream.

The hydrogenated amorphous silicon (a-Si:H) thin film control samples were fabricated via plasma enhanced chemical vapour deposition (PECVD) on crystalline silicon wafers pieces (2x2 cm^2) covered with 5µm silicon oxide. The PECVD was performed with 2% silane gas in nitrogen, 0.5 Torr pressure, 10 W power and 250°C for 10 min. The final a-Si:H film thickness was about 80 nm. With these control a-Si:H samples different experiments were performed to characterize the surfaces at critical modification stages.

The first step of the MZI sensor fabrication was the PECVD deposition of a-Si:H, such as mentioned for the control samples, on 3x3 cm^2 crystalline silicon wafer pieces covered with 5 µm silicon oxide. Then conventional lithography and reactive ion etching was performed in order to form the rib waveguide structure. The last step of the MZI sensor fabrication was the creation of a structured cladding layer with spin-coated SU-8 2002 (MicroChem, Boston, USA), which was soft baked at 95°C (1 min), exposed to UV light at 365 nm (12 s) in the mask aligner MJB3 (Suss MicroTec, Garching, Germany) by using a Chromium-cladding mask, post baked at 95°C (2 min), developed in SU-8 developer (60 s), rinsed in isopropyl alcohol and finally hard baked at 150°C (15 min).

Silanization with 3-mercaptopropyl trimethoxy silane

The fundamental silanization with 3-mercaptopropyl trimethoxy silane (MPTMS) was optimized for crystalline silicon (cSi) and hydrogenated amorphous silicon (a-Si:H). The optimized silanization protocols are listed in Table S1. For quantification, the thiol-groups of the MPTMS-derivatized surfaces were labelled with tetramethylrhodamine-5-maleimide (TMR5M). For this purpose, 10 µM TMR5M was added to 1 ml PBS buffer (5 mM, pH 7.3) with 10% (v/v) isopropyl alcohol. This solution was spotted with a pipette (5 µl) onto the MPTMS surfaces. After a reaction time of 30 min, the surfaces were washed with ultrapure water and isopropyl alcohol and dried in nitrogen stream. The fluorescence signal was measured at 532 nm excitation wavelength with the TECAN fluorescence scanner. In Table S1, measured fluorescence intensities, used photomultiplier tube (PMT) values as well as optimized parameters are summarized for each material.

The PMT value is the adjustment value for the voltage on the dynodes in the photomultiplier tube. A high PMT value means a high amplification of the fluorescence intensity and low surface density of the created functionalities.

Table S1: Overview of MPTMS silanization for different waveguide materials.

Substrate	Fluorescence intensity (a.u.)	Photomultiplier tube value (PMT)	Activation[1]	MPTMS functionalization after activation	Cleaning
a-Si:H	2393	140	3 min oxygen plasma	5% (v/v) MPTMS in THF with 0.4% (v/v) conc. HCl, 1h	5 min ultrasonic bath in isopropyl alcohol, 2x ultrapure water, 1 x 2-propanol, dried in the nitrogen stream
cSi	1014	170	10 min oxygen plasma	5% (v/v) MPTMS in THF with 0.4% (v/v) conc. HCl, 1h	

[1] The oxygen plasma activation was performed with the plasma system Femto (generator: 2.45 GHz) from Diener, Stuttgart, Germany.

Optimization of the thiol-ene click reaction

The thiol-ene click reaction was optimized on MPTMS silanized a-Si:H control samples with 10-undecenoic acid (UDA) concentration and reaction time as factors. The surface carboxylic acid groups were then modified in a following step with ethylene diamine (EDA) by using 1-ethyl-3-(3-dimethylaminopropyl)carbodiimide (EDC) chemistry [4] (20 mM EDC, and 500 mM EDA in 0.1 mM 2-(*N*-morpholino)ethanesulfonic acid buffer, pH 4.7, 2 h). Subsequently, the amino-groups were labelled with *N*-hydroxysulfosuccinimide (NHS) DyLight, in order to compare the fluorescence intensities. In Figure S2 the results obtained by TECAN fluorescence scans, with 633 nm excitation wavelength and 575 nm emission filter, are graphically illustrated. The best results were obtained with 50% UDA in methanol with 5 mg/ml 2,2-dimethoxy-2-phenylacetophenone (DMPA) and 30 min reaction time. The negative controls (same treatment but no exposure to UV light) show a significantly lower fluorescence signal (see Fig. S2).

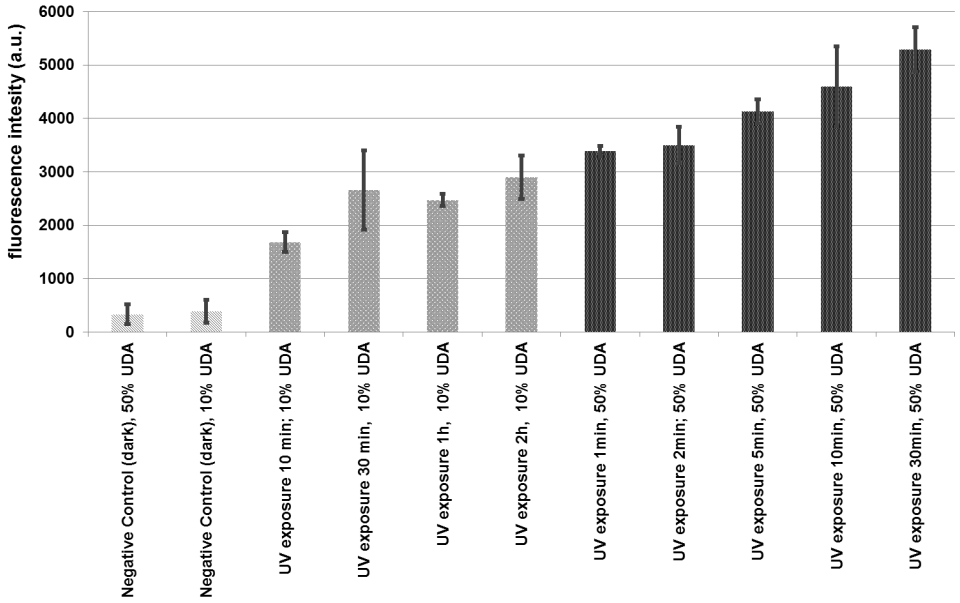

Figure S2: Results of the thiol-ene-click reaction optimization (PMT is 170)

The optimized reaction was transferred to crystalline silicon (cSi) surfaces and the results were compared with the a-Si:H surface modification by NHS-DyLight amino-group labelling. The results are depicted in Figure S3.

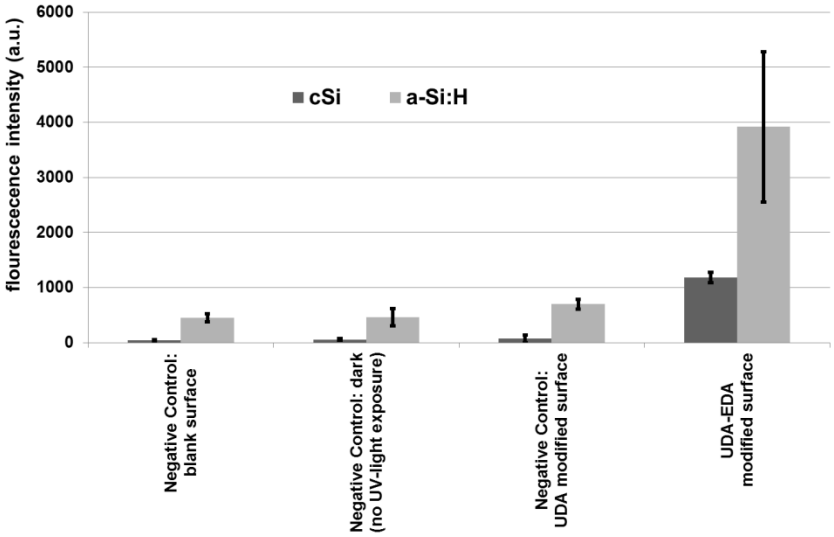

Figure S3: Comparison of optimized thiol-ene-coupling on MPTMS silanized a-Si:H and cSi surfaces. The negative controls are used include a blank (non-modified) surface, a sample that is modified without UV-light exposure in the thiol-ene coupling step, as well as a UDA-modified surface that do not carry reactive amino-groups (PMT is 170).

The cSi surfaces show a three times lower fluorescence intensity, which corresponds to a lower functional group density at the surface. Three different types of negative controls are chosen to prove the specificity of the reaction, and include blank (non-modified) surfaces, samples that are processed without UV-light exposure in the thiol-ene coupling step, as well as samples that are only modified with 10-undecenoic acid (UDA) and do not carry reactive amino-groups (see Fig. S3).

EDC Chemistry for the surface modification with polyamines

For the covalent coupling of the polyamines (viz. PMAM G1, PAMAM G5, PEI) to the carboxyl terminated surface, EDC chemistry is used. 10 µM amine-derivative is solved in 0.1 mM MES-buffer, pH 4.75, and mixed with 5 mM Sulfo-NHS, 5 mM EDC before use. After the 2 h reaction time the surfaces are washed two times with ultrapure water, 2-propanol and dried in nitrogen stream.

Biotin- and iminobiotinylation of the selected polyamines

The surfaces modified with multifunctional polymers are dipped in 40 ml borate buffer (50 mM, pH 8.5) containing 2 mg NHS-biotin or NHS-iminobiotin trifluoroacetamide (dissolved in 1 ml dimethylformamide) for 1 h at 4°C. After washing with borate buffer, the iminobiotin surfaces were dipped for another 2 h in fresh borate buffer. This step is necessary to cleave the trifluoroacetamide protection group from the guanidinium moiety of the iminobiotin residue.

Synthesis of iminobiotin-modified PEI (PEI-IB)

40 mg of 50% (v/v) aqueous solution of PEI (≈ 20 mg or 26 nM PEI) were mixed with 200 µl borate buffer (500 mM, pH 8.5) and 2.5 mg NHS-iminobiotin dissolved in 100 µl dimethyl formamide. The reaction was performed for 1 h at 4°C. To remove non-reacted iminobiotin and to hydrolyse the trifluoroacetamide protection group, the solution was dialysed 2 h against borate buffer and 12 h against 15 mM PBS buffer at pH 7.4. The final solution was diluted to a concentration of 50 µg/ml PEI-IB with 15 mM PBS buffer pH 7.4 and stored at 4°C until use.

4 XPS Spectra and Tables

XPS-Spectra of non-modified a-Si:H and cSi substrates

The full XPS spectra of non-modified a-Si:H and cSi waveguide materials are shown in Fig. S4. The nitrogen in the a-Si:H spectra originate from the PECVD process, while the carbon peak is an impurity on the a-Si:H and cSi surface.

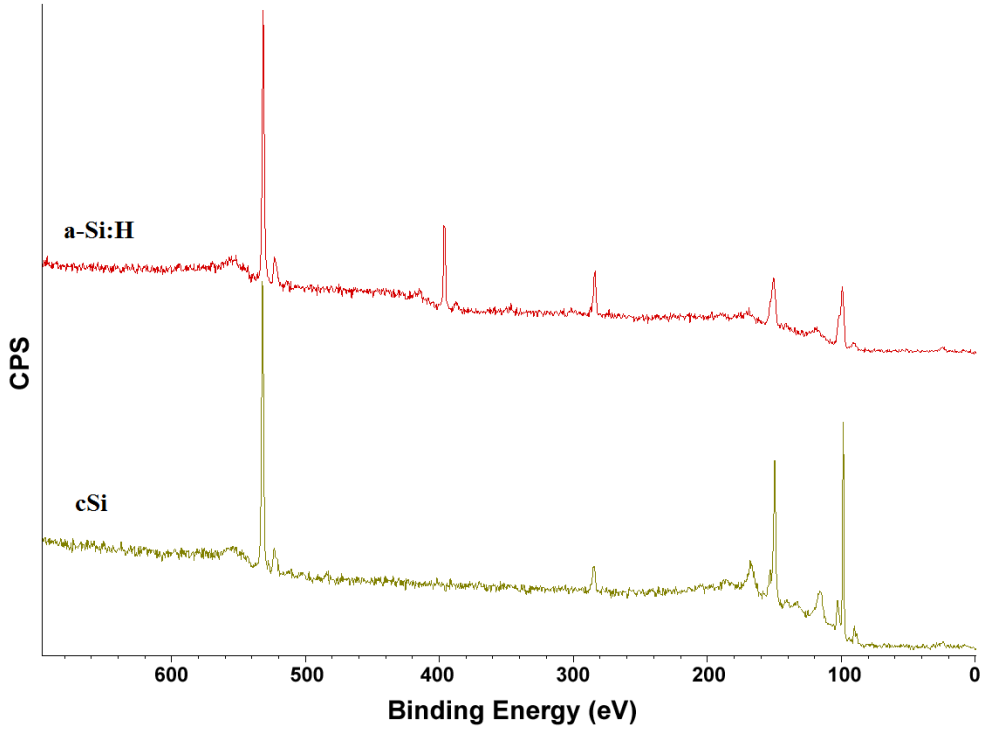

Figure S4: Full XPS spectra of non-modified a-Si:H and cSi surfaces.

In Table S2 the XPS data for all measured surfaces are summarized and in Figure S5 and Figure S6 the carbon C1s and nitrogen N1s peak deconvolution spectra are depicted. The peak mapping is performed literate supported. [5,6,7,8].

Table S2: XPS data including atomic compositions, amino-group concentration and polymer layer thickness d of EDA, PAMAM G1 and G5 and PEI surfaces

	EDA		PAMAM G1		PAMAM G5		PEI	
Atomic composition (values in %)	**a-Si:H**	**cSi**	**a-Si:H**	**cSi**	**a-Si:H**	**cSi**	**a-Si:H**	**cSi**
Si2p	37.74	49.02	33.79	39.51	27.99	31.63	27.41	34.57
O1s	36.96	35.79	32.30	32.13	31.25	32.01	26.35	30.72
C1s	13.85	12.47	20.77	24.03	26.79	30.62	30.00	26.68
N1s	11.46	2.72	13.14	4.34	13.98	5.75	16.24	8.03
N1s peak deconvolution (%)	**EDA**		**PAMAM G1**		**PAMAM G5**		**PEI**	
silicon nitride derivates Si-N (396.09 and 396.89 eV)	10.02		9.66		7.63		7.50	
secondary/tertiary amines (398.07 eV)			0.26	0.29	0.62	0.45	1.08	0.35
primary amines R-NH_2 (398.86 eV)	1.44	0.88	2.17	2.37	3.91	3.75	6.60	6.47
Amide NHC=O (400.9eV)		0.46	1.04	1.02	1.82	1.55		
Protonated amine NH_3^+ (401.73 eV)							1.08	1.22
Polymer layer thickness *d* (nm)	0.46	0.33	0.91	1.09	1.37	1.79	1.23	1.93

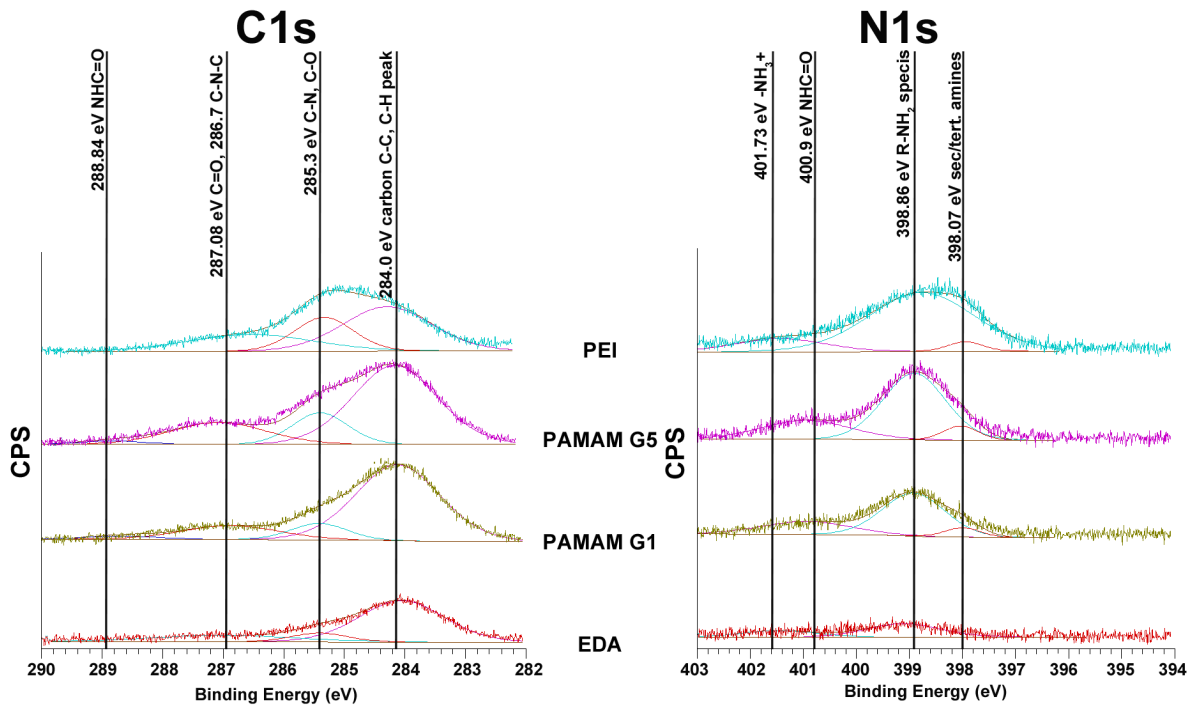

Figure S5: XPS C1s and N1s peaks of modified cSi surfaces.

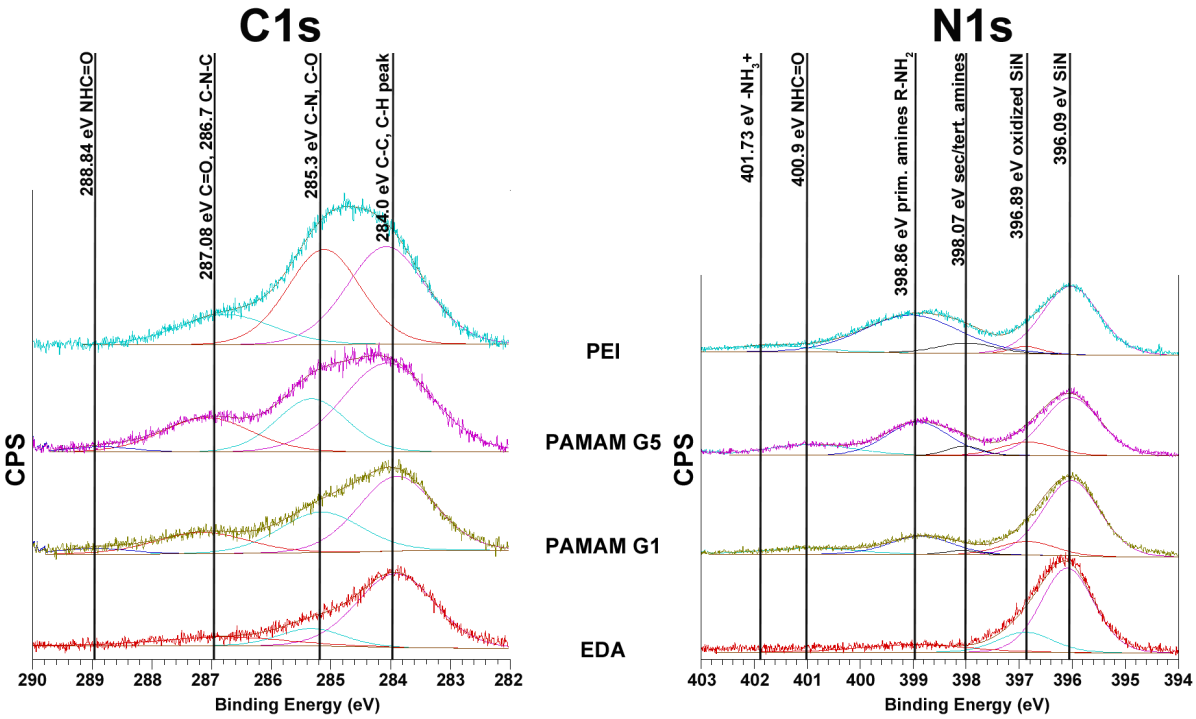

Figure S6: XPS C1s and N1s peaks of modified a-Si:H surfaces. The silicon nitride derivate peaks originates from the PECVD process.

5 Streptavidin binding kinetics

The binding kinetics of streptavidin to the iminobiotinylated MZI sensor surfaces was analyzed assuming a pseudo first order binding kinetics.

Association rate k_{on}

The following equation (2) describes the association and dissociation process of the target protein to the functionalized surface:

$$\frac{d}{\mathrm{dt}} R_t = k_{\mathrm{on}} * c * (R_{max} - R_t) - k_{\mathrm{off}} * R_t \qquad \text{(Eq. 2)}$$

R_t is the signal response at the time t, and R_{max} the maximal signal response at the sensor saturation. (R_{max}-R_t) corresponds to the number of free binding sites, and c represents the concentration of streptavidin (1666 nM). k_{on} and k_{off} are association and dissociation rate constants, respectively.

By solving the differential equation, equation (3) is obtained, which was utilized for the fitting of the streptavidin binding curve using the program *Sigmaplot* 12.5 (Systat Software Inc., Erkrath, Germany). From this fitting we obtained k_{on} values for the different iminobiotinylated surfaces based on multifunctional polymers (see Table S4).

$$\mathrm{R}_t = \frac{k_{\mathrm{on}} * c * R_{max}}{k_{\mathrm{on}} * c + k_{\mathrm{off}}} * (1 - \mathrm{e}^{-(k_{\mathrm{on}} * c + k_{\mathrm{off}}) * t}) \qquad \text{(Eq. 3)}$$

Dissociation rate k_{off}

The dissociation rate can be obtained by the real-time monitoring curve of the streptavidin dissociation from the iminobiotinylated surfaces during PBS buffer rinsing.

The solved differential equation (Eq. 4) leads to the exponential decay function of the streptavidin dissociation (Eq. 5).

$$\frac{d}{dt}R_t = -k_{off} * R_t \qquad \text{(Eq. 4)}$$

$$R_t = R_0 * e^{-(k_{off}*t)} \qquad \text{(Eq. 5)}$$

Eq. 5 was used to fit the dissociation curves of streptavidin on PAMAM G1-, PAMAM G5- and PEI-iminobiotin functionalized MZI sensors with *Mathematica* 7.0 (Wolfram Research, Oxfordshire, United Kingdom). The curves show biphasic dissociation kinetics with a fast k_{off1} and a slow k_{off2}. k_{off1} could be interpreted as the dissociation rate of streptavidin from the specific binding sites (iminobiotin), while k_{off2} could stem from slow unspecific binding or rebinding processes that slows down the dissociation of streptavidin from the iminobiotinylated polymer network.

In Fig. S7 the dissociation curve of streptavidin from the PEI-iminobiotin MZI sensor is depicted as an example for the calculations. The values for k_{off1} and k_{off2} for the iminobiotinylated multifunctional polymer-modified MZI-sensors are summarized in Table S3.

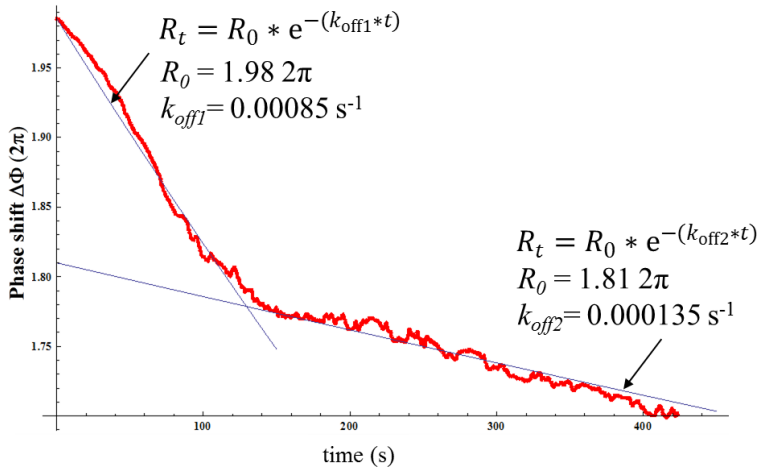

Figure S7: Dissociation curve of streptavidin from the PEI-iminobiotin MZI sensor.

Because of the negligibly small value of k_{off2}, only k_{off1} has been used for the calculation of dissociation and association constants (see Table S4).

Table S3: Values for k_{off1} and k_{off2} for the iminobiotinylated multifunctional polymer-based sensor surfaces

Multifunctional Polymer	k_{off1} (s^{-1})	k_{off2} (s^{-1})
PAMAM G1	0.0025	0.00055
PAMAM G5	0.0013	0.00015
PEI	0.00085	0.000135

Dissociation and association constants

From determined k_{on} and k_{off1} values, the streptavidin - iminobiotin dissociation ($K_D = k_{off1}/k_{on}$) and association constants ($K_A = k_{on}/k_{off1}$) can be calculated for PAMAM G1, G5 and PEI MZI sensor surfaces. In Table S4 the obtained values are summarized.

Table S4: Kinetic (k_{on}, k_{off1}) and thermodynamic (K_D, K_A) parameters of streptavidin binding to the iminobiotinylated multifunctional polymer based surfaces measured with a-Si:H MZI sensors

	PAMAM G1	PAMAM G5	PEI
k_{on} ($M^{-1} s^{-1}$)	1425.72	1331.5694	1815.0891
k_{off1} (s^{-1})	0.0025	0.0013	0.00085
K_D ($M\ L^{-1}$)	1.75E-06	1.08E-06	4.68E-07
K_A ($L\ M^{-1}$)	4.67E+05	9.28E+05	1.87E+06

6 Multilayer deposition to determine the association constant

Multilayers of up to five streptavidin/PEI-IB bilayer stacks were built up by alternating depositions employing different streptavidin concentrations (160-1666 pM/ml) at constant PEI-IB concentration (50 µg/ml). A single sensor chip was used for these experiments as it could be regenerated due to the reversibility of the streptavidin-iminobiotin interaction. Regeneration was performed by 3.5 mM HCl rinsing (5 min). In Fig. S8 the signal increase from the first until the fifth bilayer stack is depicted for different streptavidin concentrations. The sensor response increases linearly for all measured concentrations from the first until the fifth bilayer stack.

This concentration-dependent amplification was also found in previous studies with other protein deposition systems [1].

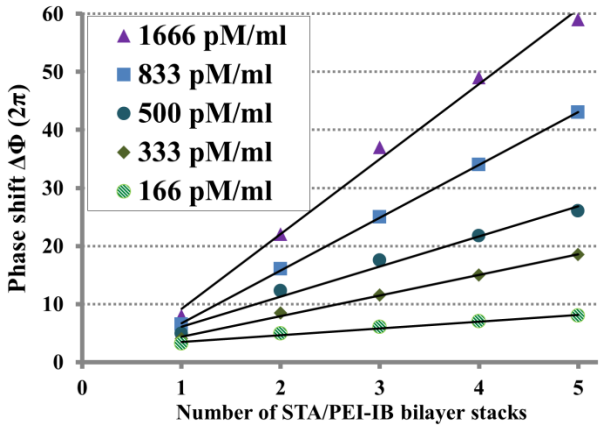

Figure S8: Phase shift plotted against the number of STA/PEI-IB bilayer stacks for different concentrations of streptavidin. The signal increases linearly for all measured streptavidin concentrations.

The association constant (K_D) is calculated by using the Langmuir isotherm (Eq. 6) and the program *Sigmaplot* 12.5 (Systat Software Inc., Erkrath, Germany). Therefore, the measured streptavidin concentrations (C) in the feed solution are plotted against the obtained sensor signal (S), and the discrete values of the maximum signal at infinitely high concentrations (S_{max}) and the dissociation constant (K_D) are obtained by curve fitting.

$$S = S_{max} * C/(K_D + C) \qquad \text{(Eq. 6)}$$

The values of K_D and K_A (=1/ K_D), as well as the according standard errors are listed in Table S5. The association constant calculated for the first bilayer deposition (K_A=2.1x10^6) is similar to the association constant calculated by using the association rate (k_{on}) and dissociation rate (k_{off1}) (K_A=1.87x10^6), shown in section five ("Streptavidin binding kinetics").

Table S5: Value of association constant K_A at different numbers of PEI-IB/STA bilayer stacks.

PEI-IB/STA bilayer stacks	K_D (M L^{-1})	Standard Error	K_A (L M^{-1})	log (K_A)
1	4.64E-07	9.60E-08	2.15E+06	6.33
2	1.01E-06	8.60E-08	9.95E+05	6.00
3	1.76E-06	2.01E-07	5.67E+05	5.75
4	1.96E-06	3.74E-07	5.11E+05	5.71
5	1.85E-06	5.32E-07	5.41E+05	5.73

7 References

1 O. Parriaux, Journal of Lightwave Technology, 1998, 16, 573-582.
2 K. Tiefenthaler, W. Lukosz, J. Opt. Soc. Am. B, 1989, 6, 209-220.
3 E. Melnik, P. Muellner, R. Bruck, .M Laemmerhofer, R. Hainberger, Optical Sensors, OSA Technical Digest (online), Optical Society of America, (2012) paper STh1B.4.
4 S. Sam, L. Touahir, J. Salvador Andresa, P. Allongue, J.-N. Chazalviel, A. C. Gouget-Laemmel, C. Henry de Villeneuve, A. Moraillon, F. Ozanam, N. Gabouze and S. Djebbar, Langmuir, 2010, 26, 809–814.
5 V. Mittal, Surface Modification of Nanotube Fillers, Wiley-VCH Verlag, Weinheim, 2011.
6 A. Ektessabi and S. Hakamata, Thin Solid Films, 2000, 377-378, 621–625.
7 C. Huang, K. G. Neoh, L. Wang, E.-T. Kang and B. Shuter, J. Mater. Chem., 2010, 20, 8512.
8 Y. Huang, J. Yang, Novel Colloidal Forming of Ceramics, Springer, 2010.